Visual effort moderates a self-correcting nonlinear postural control policy

Damian G. Kelty-Stephen[1], I-Chieh Lee[2], Nicole S. Carver[3], Karl M. Newell[4], and Madhur Mangalam[5]

[1]Department of Psychology, Grinnell College, Grinnell, IA 50112, USA

[2]UNC-NC State Joint Department of Biomedical Engineering, UNC-Chapel Hill, Chapel Hill, NC 27514, USA

[3]Department of Psychology, University of Cincinnati, Cincinnati, Ohio, United States of America

[4]Department of Kinesiology, University of Georgia, Athens, GA 30602, USA

[5]Department of Physical Therapy, Movement and Rehabilitation Sciences, Northeastern University, Boston, MA 02115, USA

Author for correspondence:

Damian G. Kelty-Stephen

e-mail: keltysda@grinnell.edu

Madhur Mangalam

e-mail: m.mangalam@northeastern.edu

Ethics statement. The present study was approved by the Institutional Review Board (IRB) at the University of Georgia (Athens, GA). All participants provided verbal and written informed consent before participation.

Data accessibility. All data analyzed in the present study are available upon request.

Author contributions: D.G.K-S., I.-C.L., K.M.N., and M.M. conceived and designed research; I.-C.L. performed experiments; D.G.K-S., N.S.C., and M.M. analyzed data; D.G.K-S. and M.M. interpreted results of experiments; M.M. prepared figures; D.G.K-S. and M.M. drafted manuscript; D.G.K-S., I.-C.L., K.M.N., and M.M. edited and revised manuscript; D.G.K-S., I.-C.L., N.S.C., K.M.N., and M.M. approved final version of manuscript.

Competing interests. Data available as part of the electronic supplementary material.

Abstract

A growing consensus across otherwise disparate perspectives on perception and action is that visually guided postural control emerges from within task constraints. Task constraints generate physiological fluctuations across various parts of the body. These fluctuations foster exploration of the available sensory information. For instance, standard deviation (*SD*) and temporal correlations of bodily sway can indicate how richly postural control samples available mechanical and visual information. Too much or too little *SD* entails destabilization of posture. Temporal correlations show a similar relationship, but they have also been shown to support carrying sampled information to other aspects of the postural system. The present study shows that increasing visual constraints on posture reveals an adaptive relationship between *SD* and temporal correlations of postural fluctuations. In short, changing the viewing distance of a fixation target shows that temporal correlations self-correct themselves across time and diminish *SD* across time as well. Notably, these relationships were strong for all viewing distances except the most comfortable viewing and reaching distance. This self-correcting relationship allows the visual layout itself to press the postural system into a poise for engaging with objects and events in the surrounding.

Keywords: biotensegrity, center of mass, center of pressure, fractality, Hurst's exponent, postural sway

1. Introduction

1.1. Stability of suprapostural visual activities at longer scales rests on fluctuating behavior at shorter scales

Standing quietly and maintaining focus on a target in front of us is the preamble to very many coordinated behaviors—we might lean forward and reach or track the target's progress and bat it away. However, this starting position is not merely the preamble to action but is already a rich wellspring of the action itself, exhibiting a continuous stream of intermittent fluctuations. We can see these fluctuations in our bodily center of mass (CoM) and center of pressure (CoP), where ground reaction forces meet our lower extremities. So long as they do not pitch the CoP beyond the base of support, these fluctuations are crucial to maintaining a quiet stance [1,2]. This variability offers the body a subtle and flexible command of the mechanical surface underfoot [3,4], exemplifying long-respected proposals that noise can stabilize nonlinear-dynamical systems [5,6].

Lacing our postural system into our visual field are eyes, moving to lock focus on a distal point in the world. Admittedly, maintaining focus involves "fixations" of the eyes no less than upright posture can seem "still," but this fixation is not stasis: fixations are regularly recognized as a class of movement [7] consisting of a vibrant, fluctuating foundation of smaller movements called "microsaccades" [8]. These microsaccades serve to stabilize images that would otherwise fade on a static retina [9], thus playing a similar role to the visual system that fluctuations play for the postural system. Indeed the exploratory role of fluctuating movements extends to the extremities of the body besides and intermediating between upright posture and vision [10], suggesting a strong role for postural sway in supporting visual perception [11–13]. Thus, even when standing quietly upright while fixating at a visual target, the body is coursing with fluctuations ferrying information across the body.

The present work aims to explore how visual effort might affect how fluctuations flow within the bodywide postural system. Postural fluctuations produce translations and rotations of visible surfaces specific to the spatial relationships of the objects in the visual field. These movement-induced translations and rotations compose an optic flow that provides visual support for the subsequent movement. Thus, subtle postural sway offers the sighted organism a rich source of information about the layout of objects in the visual field. The visual layout itself then presses the postural system into a poise for engaging with objects and events in the surrounding. Visual targets appearing closer to or farther from the looking postural system impose retina-specific constraints of oculomotor convergence [14,15] and chromatic aberration [16]. Consequently, changes in a target's size relative to other aspects of the visual field entails changes in optic flow (figure 1). These multi-scale factors affect postural stability, reflecting changes in postural configurations and hence in the flow of information needed to organize these postures.

1.2. Perceptual constraints on postural stability could reshape intrapostural interactivity

In the present study, we aim to explore how changing the viewing distance might change how the postural system exchanges fluctuations within and between CoM and CoP. We examined the relationship between bulk variability in CoP fluctuations (i.e., standard deviation, *SD*) and temporal structure (i.e., fractal scaling, *H*) in CoM and CoP fluctuations. The implication of *SD* is the prevailing tradition, but that of fractality rests on two until-recently parallel bodies of evidence, one specifically requiring variations in fractal geometry for modeling the bodywide organization of the movement system and the second suggesting that

capacity of bodily fluctuations to ferry information inheres at least partially in its fractal structure. Movement depends on the bodywide network of connective tissues and nervous tissues, forming flexible relationships that balance tensions with compressions at multiple scales of analysis [17–23]. This organization entails a specifically multifractal geometry that embodies multiple scale-invariant patterns of behavior (e.g., microsaccades within the saccades that intersperse larger saccades by the eye and turns by the head) across time and across space. CoP fractality has repeatedly borne a consistent relationship to perceptual judgments of visual and haptic stimuli [24–29], and research into perceptual tasks (e.g., manually wielding an object to judge heaviness or length) while standing shows that a bodywide flow of fractal fluctuations precedes and shapes the verbal articulation of perceptual judgments [30,31]. Hence, a fractal flow within posture seems to support information flow and might provide a glimpse of the control policy emerging from bodily situation in task constraints.

1.3. Visual effort for fixating across different viewing distances could reveal different relationships amongst CoM fractality, CoP fractality, and CoP *SD*

1.3.1. The task

The present work is a reanalysis of a previous study that manipulated viewing distance while measuring CoM and CoP [32]. Healthy adults stood maintained a quiet stance under six different conditions: a control condition with eyes closed and five conditions with eyes open and fixating on a red laser point projected on surfaces at 20, 50, 135, 220, and 305 cm distance. We reanalyzed these data by carving individual trials under each viewing condition into non-overlapping sub-trial segments, estimating fractal scaling and *SD* within each segment, and using vector autoregression (VAR) modeling to test the interactions among these descriptors across segments within each trial.

1.3.2. The hypotheses

Hypothesis 1: Weaker intrapostural interactivity while standing quietly with eyes closed.

First, respecting the evidence that maintaining fixation recruits oculomotor effort that can perturb posture [33,34], we predicted that the addition of a fixation task to quiet standing would generally accentuate intrapostural interactivity, suggesting that standing quietly with eyes closed would show weaker evidence of intrapostural interactivity.

Hypothesis 2: Resemblance between the 50-cm viewing condition and the eyes-closed condition.

The 50-cm viewing distance is within the comfortable viewing distance, ideal for the human eyes' focus of red light [16], as well as ideal for requiring the least straining oculomotor convergence [14,15]. Hence, our last and most specific prediction was that the 50-cm viewing condition would yield intrapostural interactivity most closely resembling that in the eyes-closed condition. That is, because 50-cm requires the least visual strain, the effects among CoM fractality, CoP fractality, and CoP *SD* would show the least differences from the eye-closed condition.

Hypothesis 3: Self-correction of fractality across 10-s segments.

Postural sway is more correlated at short timescales on the order of 10 s and more anticorrelated over longer timescales [35]. For instance, posture roams freely about a fixed average CoP position but self-corrects at the margins of the base of support to maintain a quiet stance [35–37]. In this sense, we predicted that fractality itself would show similar self-

corrections over time, with prior increases in fractality followed by subsequent alternating decreases and increases in fractality. This self-correcting feature would be a crucial part of any control in which temporal correlations stabilize sway.

Hypothesis 4: Inverse relationship between fractality and SD across 10-s segments.

Because fractality entails long-range temporally organized responsivity to mechanical perturbations [38,39], we expected an inverse relationship between either or both of CoP and CoM fractality and CoP *SD*. That is, increases in CoP and CoM fractality would predict later decreases in CoP *SD* (Hypothesis 4a), as well as increases in CoP-*SD* would predict later decreases in CoP and CoM fractality (Hypothesis 4b). This feature could reflect a second key component of task-dependent emergent postural control.

2. Materials and methods

2.1. Participants

Seven adult men and nine adult women (*M*±1*SD* age = 23.8±3.9 years) without any skeletal or neuromuscular disorder voluntarily participated after providing verbal and written consent approved by the Institutional Review Board (IRB) at the University of Georgia (Athens, GA).

2.2. Experimental task and procedure

Each participant stood barefoot with one foot on each of two force plates (AMTI Inc., Watertown, MA), 25 cm apart (figure 1*a*). From behind the participant, a laser pen projected a static point-light on the center of a 5×5" white tripod-mounted screen in front of a white visual-field-filling background. The two force plates measured 3D moments and ground reaction forces. The full-body motion of each participant was measured using VICON Plug-in Gait full-body 39 marker set and an 8-camera VICON motion tracking system (VICON Inc., Los Angeles, CA). The kinetic and kinematic data were synchronized and sampled at 100 Hz.

Each participant was instructed to maintain a quiet stance for 120 s under six different viewing conditions: eyes closed and while fixating visually on the point-light point positioned at 25, 50, 135, 220, and 305 cm distance in front. Each participant completed 18 trials (6 conditions × 3 trials) in a single 90-min session with randomized trial order and with breaks on request and between every six trials.

2.3. Data processing

All data processing was performed in MATLAB 2019b (Matlab Inc., Natick, MA). The position of the bodily center of mass (CoM) was estimated by submitting segment lengths of the head, trunk, pelvis, and left and right hand, forearm, upper arm, thigh, shank and foot to the equations provided by Zatsiorsky and Seluyanov [40], which yielded a 3D center of pressure (CoP) series describing CoM position along the participant's anterior-posterior (AP), medial-lateral (ML), and superior-inferior axes. 3D moments and ground reaction forces measured on each trial yielded a 2D center of pressure (CoP) series describing CoP position along the participant's AP and ML axes. Over 120 s duration, each trial yielded a 3D CoM series and a 2D CoP series each of 120 s or 12000 samples, divided into 12 segments of 10 s or 1000 samples each. Each segment yielded two 999-sample one-dimensional series: a CoM spatial Euclidean displacement (SED) series describing the amplitude of CoM displacement (figures 2*a* to 2*f*) and a CoP planar Euclidean displacement (PED) series describing the amplitude of CoP displacement (figures 2*a* to 2*f*).

2.4. Detrended fluctuation analysis (DFA)

DFA estimates Hurst's exponent, H, describing the growth of root mean square (RMS) fluctuations with time for first-order displacements known as fractional Gaussian noises (fGn) [41,42]. First, it integrates time series $x(t)$ with N samples to produce $y(t)$:

$$y(t)=\sum_{i=1}^{N} x(t)-\overline{x(t)} \quad .$$

Next, DFA computes RMS residuals from the linear trend $y_n(t)$ over nonoverlapping *n*-length bins of $y(t)$ to build a fluctuation function $f(N)$:

$$f(N)=\sqrt{(1/N)\sum_{i=1}^{N}(x(t)-\overline{x(t)})^2} \quad ,$$

for $n<N/4$. On standard scales, $f(N)$ is a power law:

$$f(N)\sim n^H \quad ,$$

where H is the scaling exponent. H is estimated as the slope of $f(N)$ in log-log plots:

$$\log f(N)=H\log(n) \quad .$$

DFA estimated H_{fGn} for the original version (i.e., unshuffled) and a shuffled version (i.e., a version with the temporal information destroyed) of each CoM SED series (CoM-H_{fGn}) and CoP PED series (CoP-H_{fGn}) over the following bin sizes: 4, 8, 12,… 128; figures 2*g* and 2*h*).

2.5. Vector autoregression (VAR) analysis

VAR captures linear interdependencies amongst concurrent series and here modeled intrapostural effects of CoM-H_{fGn}, CoP-H_{fGn}, and CoP-*SD* in one segment on CoM-H_{fGn}, CoP-H_{fGn}, and CoP-*SD* in subsequent segments (figure 3). VAR describes each variable based on its own lagged value and that of each other variable. Lag is ideally increased until the residuals appear independently and are distributed identically [43].

VAR allows forecasting unique effects of endogenous variables on later values of each other through impulse-response functions (IRFs). IRFs evaluate the relationship between $f(t)$ and $g(t+\tau)$, or between $g(t)$ and $f(t+\tau)$, where τ is a whole number corresponding to a segment within a trial. Provided VAR residuals are independent and identically distributed (i.i.d.), orthongonalizing these residuals allows simulating an "impulse" to the system by adding 1SEM to any single variable, and using VAR coefficients to describe propagation of later "responses" across all endogenous variables. The IRF describes how an impulse in one series changes later predicted values in a different time series [44,45]. All VAR models converged with lag 1, with residuals passing all tests for i.i.d. status. We performed VAR analysis using the *vars* package in RStudio [46].

2.6. Statistical analysis of pairwise IRFs

A regression model [47] treated IRFs between each pair of postural descriptors as the dependent measure and tested the effect of predictors including the full-factorial set Trial × Segment × Impulse × Response using the *nlme* package for RStudio [48]. Impulse and Response served as class variables encoding the different descriptors (CoP-H_{fGn} and CoM-H_{fGn}, and CoP-*SD*) serving as impulse and as response variables, respectively. Orthogonal linear, quadratic, and cubic polynomials of Segment modeled how impulse-response

relationships changed over 999-sample segments within a trial. We used the cubic polynomial to capture the general nonlinear decay of IRFs across later segments. The interactions of H_{fGn} or *SD* with Segment indicated changes in these effects with different third-order polynomial responses over subsequent trials. The Impulse × Response terms highlighted significant differences of specific impulse-response pairs from the global patterns.

3. Results

3.1 CoM and CoP showed fractal fluctuations

H_{fGn} for all original series fell in the fractal range ($0.5 < H_{fGn} < 1$; figures 2*g* and 2*h*) and significantly exceeded for all corresponding shuffled series (*p*s < 0.0001; table S1), indicating fractal fluctuation in both CoM and CoP. Crossovers between shorter- (bin sizes: 4, 8, 12,… 64) and longer-scale (bin sizes: 4, 8, 12,… 128) behavior exhibited no reliable differences, as H_{fGn} estimates from only shorter-scale behavior correlated strongly with H_{fGn} estimates from the entire DFA fluctuation function (CoM: Spearman's *ρ*s = 0.96, 0.91, 0.94, 0.94, 0.93, and 0.94 for the eyes-closed and the 25-, 50-, 135-, 220-, and 305-cm eyes-open conditions, respectively, *p*s < 0.0001); CoP: *ρ*s = 0.96, 0.89, 0.93, 0.92, 0.91, and 0.94, *p*s < 0.0001).

3.2. Maintaining a quiet stance with eyes closed weakened intrapostural interactivity with trials (Hypothesis 1)

When maintaining a quiet stance with eyes closed, prior increases in CoM-H_{fGn} showed no significant later CoP-*SD* responses and only subtle later CoP-H_{fGn} and CoM-H_{fGn} responses (figures 4*a* and 4*b*). Regression modeling of IRFs (table S2) showed that increases in CoM-H_{fGn} preceded a short-term subsequent decrease and slow, nonlinear rebound (Segment(Quad): $b = -6.19\times10^{-1}$, $p = 0.017$; and Segment(Cubic): $b = 5.36\times10^{-1}$, $p = 0.040$) in all variables except CoP-*SD* (Segment(Quad) × Response(CoP-*SD*): $b = 6.21\times10^{-1}$, $p = 0.092$). This decrease-and-nonlinear-rebound was canceled out with Trial for later CoM-H_{fGn} responses (Trial × Segment(Quad): $b = 4.29\times10^{-1}$, $p < 0.001$; Trial × Segment(Cubic): $b = -3.27\times10^{-1}$, $p = 0.007$) but showed no such change for later CoP-H_{fGn} responses (Trial × Segment(Quad) × Response(CoP-H_{fGn}): $b = -4.04\times10^{-1}$, $p = 0.018$; and Trial × Segment(Cubic) × Response(CoP-H_{fGn}): $b = 3.45\times10^{-1}$, $p = 0.042$) and CoP-*SD* responses (Trial × Segment(Quad) × Response(CoP-*SD*): $b = -4.27\times10^{-1}$, $p = 0.012$; and Trial × Segment(Cubic) × Response(CoP-*SD*): $b = 3.28\times10^{-1}$, $p = 0.054$).

Closing eyes weakened the responsivity of all measures to prior increases in each other and in CoM-H_{fGn}, amounting to no later effects of *SD* and vanishing effects of CoP-H_{fGn} with Trial (figure 4*c* and 4*d*). Specifically, regression terms canceled out and reversed effects of prior increases of CoP-*SD* (Segment(Quad) × Impulse(CoP-*SD*): $b = 7.95\times10^{-1}$, $p = 0.031$) and CoP-H_{fGn} (Segment(Quad) × Impulse(CoP-H_{fGn}): $b = 1.35\times10^{0}$, $p < 0.001$). The eyes-closed condition did show positive effects of prior increases in CoP-H_{fGn} on later effects decaying slowly with Segment (Segment(Linear) × Impulse(CoP-H_{fGn}): $b = -7.05\times10^{-1}$, $p = 0.056$; and Segment(Quad) × Impulse(CoP-H_{fGn}): $b = 1.35\times10^{0}$, $p < 0.0001$), but this effect disappeared with Trial (Trial × Segment(Linear) × Impulse(CoP-H_{fGn}): $b = 4.86\times10^{-1}$, $p = 0.004$; Trial × Segment(Quad) × Impulse(CoP-H_{fGn}): $b = -1.04\times10^{0}$, $p < 0.0001$).

Critically, the eyes-closed condition diminished intrapostural interactions between CoP-H_{fGn} and CoP-*SD*, leaving CoP-*SD* to predict much of the later behavior elsewhere. All significant interactions involving Impulse(CoP-H_{fGn}) and Response(CoP-*SD*) significantly canceled out the corresponding lower-order interactions of Impulse(CoP-H_{fGn}), effectively

muting the effects of a prior CoP-H_{fGn} impulse on later CoP-*SD* responses [e.g., Segment(Quad) × Impulse(CoP-H_{fGn}) × Response(CoP-*SD*): $b = –1.36×10^{0}$, $p = 0.009$; Trial × Segment(Linear) × Impulse(CoP-H_{fGn}) × Response(CoP-*SD*): $b = –4.81×10^{–1}$, $p = 0.046$; Trial × Segment(Quad) × Impulse(CoP-H_{fGn}) × Response(CoP-*SD*): $b = 1.04×10^{0}$, $p < 0.0001$]. Effects promoting greater CoP-H_{fGn} at first generally vanished with Trial (Trial × Segment(Linear) × Impulse(CoP-H_{fGn}) × Response(CoP-H_{fGn}): $b = –5.54×10^{–1}$, $p = 0.021$; Trial × Segment(Quad) × Impulse(CoP-H_{fGn}) × Response(CoP- H_{fGn}): $b = –1.55×10^{0}$, $p = 0.003$). Across trials, prior increases in CoP-*SD* exerted a weaker decrease-and-nonlinear-rebound form on later CoM-H_{fGn} responses (Trial × Segment(Quad) × Impulse(CoP-*SD*): $b = –5.50×10^{–1}$, $p = 0.001$; and Trial × Segment(Cubic) × Impulse(CoP-*SD*): $b = 3.02×10^{0}$, $p = 0.077$) but retained this later effect on CoM-H_{fGn} (Trial × Segment(Quad) × Impulse(CoP-*SD*) × Response(CoP- CoM-H_{fGn}): $b = 5.37×10^{–1}$, $p = 0.023$) and on itself (Trial × Segment(Quad) × Impulse(CoP-*SD*) × Response(CoP-*SD*): $b = 5.48×10^{–1}$, $p = 0.023$).

Though not pictured here, this latter effect held robustly across all viewing conditions: prior increases in CoP-*SD* predicted later increases in CoP-*SD*, with the size of this later increase dwindling quadratically at a decreasing rate with Segment (table S2).

3.3. Intrapostural interactivity in the 50-cm viewing condition resembled that in the eyes-closed condition than that in other viewing conditions (Hypothesis 3)

Visually fixating at 50 cm elicited the least amount of intrapostural interactivity, closely resembling the eyes-closed condition. This point is evident first in terms of the number of significant effects. For instance, the regression model yielded 72 coefficients for each condition (tables S2–S6). Compared to effects for all other eyes-open conditions, the 50-cm condition showed significant but opposite effects of Segment(Linear), Trial × Segment(Linear), and Trial × Segment(Linear) × Response(CoP-*SD*) from the 135-cm condition (table S3), and a significant but opposite effect of Trial × Segment(Linear) × Response(CoP-$H_{fGn)}$ from all other eyes-open conditions (table S4). Of the remaining nine significant effects, Impulse(CoP-H_{fGn}), Segment(Linear) × Impulse(CoP-*SD*) and Trial × Impulse(CoP-H_{fGn}) did not show significance in any other eyes-open condition, and one other followed the same sign but was little more than half as large as the same significant effect for all other eyes-open conditions (table S4).

In short, these distinctions entailed that, with Trial, the 50-cm condition showed greater but shorter-term reductions in *SD* following increases in CoP-H_{fGn}, for instance, more negative change in CoP-*SD* with Trial (Trial × Impulse(CoP-H_{fGn}) × Response(CoP-*SD*): $b = –4.98×10^{–3}$, $p = 0.023$; table S6) and stronger subsequent positive linear growth in CoP-*SD* (Trial × Segment(Linear) × Impulse(CoP-H_{fGn}): $b = 4.87×10^{–1}$, $p = 0.043$; table S4) than in other eyes-open conditions. The other eyes-open conditions typically showed a decrease in CoP-*SD* following an increase in CoP-H_{fGn}, but the subsequent rebound of CoP-H_{fGn} to zero change was slower and more nonlinear with Trial (Trial × Segment(Quad) × Impulse(CoP-H_{fGn}) × Response(CoP-*SD*): *b*s = $–1.19×10^{0}$, $–9.22×10^{–1}$, $–1.17×10^{0}$, and $–1.12×10^{0}$ for the 20-, 135-, 220-, and 305- cm conditions, respectively, *p*s < 0.01; table S4). Critically, the 50-cm condition was the only condition that did not show this change in the nonlinearity of later responses in CoP-*SD*.

3.4. CoM-H_{fGn} and CoP-H_{fGn} self-corrected from segment to segment within a trial but showed sparse effects on each other (Hypothesis 3)

In the eyes-open conditions, increases in CoM-H_{fGn} and CoP-H_{fGn} (CoM-H_{fGn} and CoP-H_{fGn}, respectively) predicted later increases and decreases in alternation over subsequent

segments (tables S2 and S5; figures 4*a* and 4*d*), suggesting that the eyes-open conditions prompted a sort of self-correcting maintenance of fractality within CoM and CoP. Thus, the act of visually fixating prompted fractality to fall in and out of zero change or to cycle around zero change with negative and positive changes following each other. The model did not yield significant IRF relationships between CoM-H_{fGn} and CoP-H_{fGn} (table S2; figures 4*b*, *c*): only the 220-cm viewing condition was accompanied by a CoM-H_{fGn} impulse that predicted later CoP-H_{fGn} responses (figure 4*d*).

3.5. Increases in CoP-H_{fGn} and CoP-*SD* predicted subsequent decreases in each other with trials (Hypothesis 4)

In the eyes-open conditions, prior impulses in CoP-H_{fGn} and CoP-*SD* both predicted later decreases in CoP-*SD* and CoP-H_{fGn}, respectively (figure 5; table S5). These IRF relationships remained robust with Trial, more so for the effects of a prior CoP-*SD* impulse on later CoP-H_{fGn} responses (figure 5*a*) than for the effects of a prior CoP-H_{fGn} impulse on later CoP-*SD* responses (figure 5*b*). The 305-cm viewing condition failed to show a significant relationship between a prior CoP-*SD* impulse and later CoP-H_{fGn} responses on only one trial. The 25-, 135-, and 220-cm conditions each exhibited one, one, and two trials, respectively, that failed to show a relationship between a prior CoP-H_{fGn} impulse and later CoP-*SD* responses.

4. Discussion

We tested four specific hypothesis concerning how visual effort might moderate intrapostural interactivity. First, we predicted that standing quietly with eyes closed would exhibit weaker intrapostural interactivity (Hypothesis 1). Second, we predicted that CoM-H_{fGn} and CoP-H_{fGn} would self-correct over time (Hypothesis 2). Third, we predicted an inverse relationship between *SD* and fractality over time, that is, that increases in CoM-H_{fGn} and CoP-H_{fGn} would prompt later decreases in CoP-*SD* (Hypothesis 3a) and that increases in CoP-*SD* would prompt later decreases in CoM-H_{fGn} and CoP-H_{fGn} (Hypothesis 3b). Fourth, we predicted that these intrapostural interactions in the 50-cm viewing condition would most closely resemble intrapostural interactions in the eyes-closed condition (Hypothesis 4). Results supported all four hypotheses with the only exception being the failure of CoM-H_{fGn} to participate in the relationships predicted in Hypothesis 3.

The regression modeling of IRFs revealed that in the eyes-closed condition, most effects of CoM-H_{fGn}, CoP-H_{fGn}, and CoP-*SD* on themselves and on each other were brief and canceled out with Segment and Trial (Hypothesis 1). Figures 4 and 5 show that IRF modeling did yield some significant later responses, but the non-significant coefficients yielded by the model reflect the fact that these significant responses were sparse and unstable.

CoM-H_{fGn} and CoP-H_{fGn} did indeed self-correct (Hypothesis 2), with zig-zag IRF plots indicating alternation between temporal correlations (i.e., persistence) and anticorrelations (i.e., antipersistence) or at least between varying degrees of temporally correlated persistence. These switches occurred as quickly as from one 10-s segment to the next, but this lag-1-segment relationship was not uniform across time or conditions (figures 4*a* and 4*c*). This finding resonates with the canonical idea that sway shows short-term persistence followed by long-term antipersistence [35,36]. The variation from greater or lesser temporal correlations from segment to segment is fleeting. These zig-zag IRF plots may reflect, first, greater persistence of sway within the base of support's canter and, second, braking or reversing by the postural control system as it approaches the margins of the base of support

[1,2]. However, testing this spatial interpretation would benefit from "rambling-trembling" frameworks that recognize a slow-moving reference point anchoring CoP within the base of support [49,50]. These findings thus warrant further investigations into how visual information moderates the rambling-trembling aspects of posture (e.g., [50,51]).

The 50-cm viewing condition yielded intrapostural interactivity that most closely resembled that in the eyes-closed condition (Hypothesis 3). The effects between CoP-*SD* and CoP-H_{fGn} in the 50-cm condition gradually decayed across trials (figure 5). These effects did not show up in every trial for all other viewing conditions, but the regression coefficient found significant nonzero effects between fractality and *SD* for all other viewing conditions and only predicted the canceling out of these effects for 50-cm condition. Hence, the viewing distances known to strain oculomotor convergence [14,15] prompted less of the intrapostural relationships that supported posture at other viewing distances. Additionally, the predicted effects of *SD* on later fractality were robust for all trials across all condition, and those of fractality on later *SD* were less robust for the 135- and 220-cm conditions. This latter difference indicates that, to some extent, targets at medium distances beyond the comfortable viewing distance might also stabilize posture [52].

Prior increases in CoP-*SD* and CoP-H_{fGn} predicted later decreases in CoP-*SD* and CoP-H_{fGn}, respectively (Hypothesis 4). As noted in Results for Hypothesis 1, prior increases in CoP-*SD* predicted later increases in itself with Segment, thus showing none of the self-corrective aspects shown by CoP-H_{fGn}. Hence, increase in CoP-*SD* predicted both later increases in CoP-*SD* and later decreases in CoP-H_{fGn}, and increases in CoP-H_{fGn} predicted later decreases in both CoP-*SD* and CoP-H_{fGn}.

4.2. Glimpses of a possible control policy for visually guided quiet stance

The present results offer insights into a possible control policy for postural stability that balances CoP-H_{fGn} with an excess of CoP-*SD*. If left to *SD* alone, posture would lean towards higher variability without clear bound: any increase in *SD* would predict later increases, and those later increases would predict even later increases, and so on. The predicted later decreases in fractality would then only serve to promote greater *SD*. It is only the corrective aspect of fractality that might allow posture to rein in the apparently self-promoting and unbounded *SD*. For instance, any decreases in fractality following increases in *SD* might trigger subsequent increases in fractality that would induce a negative check on *SD*. This causal interpretation aims only to offer a possible control policy that these results could reflect. Such causal interpretation warrants manipulations of *SD* and fractality of CoP fluctuations (if only indirectly) through a balance board or vibrotactile stimulation.

The present results from VAR analysis examining relationships between earlier impulses and later responses raise new questions for future work. For instance, past work involving explicit feedback to participants completing a motor task found that performance feedback weakened temporal correlations in movement variability in the task [53–55]. In the task of counting seconds by tapping a finger [53], the feedback provided with each tap allowed participants to offset deviations in a way that prevented errors from propagating from one tap to the next. At first glance, this finding seems at odds with the present finding that better performance—standing more quietly with less *SD*—would follow from and contribute to stronger and not weaker temporal correlations. However, it is possible that, in postural tasks, greater sway is endogenous, implicit feedback that signals the postural control system that corrections are appropriately implemented. In this way, if some proportion of *SD* reflects sway that triggers postural corrections (e.g., [56]), then the present findings would align with past findings of feedback decorrelating movement variability.

This proposed control policy may resolve long-standing questions about how fluctuations support movement stability—explicitly speaking to the "loss of complexity" hypothesis that fractal sway might be the signature of stability, suggestive of young, healthy, and typically developing physiology. This hypothesis has proven provocative but controversial. Indeed, exploratory clinical research found that temporal correlations might wander within but also beyond the fractal range. But the clinical implications were mixed, with some results indicating stronger temporal correlations in sway for younger, healthier and more typically developing participants [38,57] and other results indicating the opposite [57–59]. Meanwhile, experimental work applying "white-noise"—that is, temporally uncorrelated—mechanical vibration to the feet found that this, by definition, non-fractal and so non-complex signal stabilized sway [60,61]. In finding that greater temporal correlations were associated with later decreases in *SD* of sway, the present results align well with only half of the exploratory evidence and poorly with the finding that uncorrelated stimulation reduced sway.

Making matters seem even more paradoxical, results have curiously diverged within the same research paradigms in this vein. A reanalysis of Priplata et al.'s [61] data yielded two details [62]. Firstly, white-noise stimulation reduced temporal correlations in sway. So, in the case of unhealthy level of complexity, decorrelating overly correlated fluctuations may be an effective clinical strategy. However, secondly and less straightforwardly, the reanalysis showed that white-noise stimulation elicited stronger reduction of sway for participants exhibiting stronger temporal correlations. In a sense, white-noise stimulation seems to wipe out its efficacy by counteracting the very conditions of endogenous postural fluctuations that give it a stabilizing effect. This self-nullifying aspect of the stimulation seemed quite puzzling.

The present work solves some of this puzzle. All past work sought to find predictive effects of fluctuation patterns by associating concurrent variables: temporal correlations and sway variability for the same postural measurement series. The major contributions of examining prior effects and later responses are twofold: first, fractal temporal correlations self-correct, and second, stronger temporal correlations reduce CoP-*SD*. Together, these two points provide a framework in which the present findings align neatly with research on white-noise stimulation stabilizing posture [60,61] and to explain how fractal temporal correlations could be sometimes stabilizing and sometimes destabilizing.

Self-correction of fractal temporal correlations has been the key feature missing from the portrayal of postural stability until now. If fractal temporal correlations did not self-correct, then *SD* would increase or decrease unchecked, subverting postural stability [3,4]. Lack of self-correction in temporal correlations would mean that temporal correlations and *SD* might push each other to opposite extremes. Posture lacking sufficient variability would be unstable and overly temporally correlated; posture having too much variability would be unstable and have too little temporal correlations. Understanding self-correction in temporal correlations might then be one of the key directions for future work. Differences is temporal correlations are well-known [35,36] and often replicated [37]. The novelty lies in recognizing that weaker temporal correlations in longer timescales may hold only on average, consisting of shorter-timescale ebbing and flowing of temporal correlations. Across 10-s segments within a single trial, the VAR found a sequence of fleeting (e.g., 10-s) bouts of postural sway predicting later alternations between more or less temporal correlations.

The exact basis of this alternation of temporal correlations warrants further investigation. The question of whether these spatial constraints govern temporal correlations' self-correction would benefit from rigorous test in the "rambling-trembling" framework. This framework recognizes that the fixed reference point anchoring CoP within the base of support

drifts slowly. Thus, it is important to model the rise and fall of temporal correlations as a function of the distance between the fixed reference point and the edges of the base of support. The space that "rambling" leaves open for stable, "trembling" may govern how quickly temporal correlations alternate. Such modeling could add to the ongoing elaborations of the rambling-trembling framework to include visual constraints [50,51].

We do mean this proposal to only serve as a glimpse of what needs further validation. Naturally, the correlational analysis results are prone to mischaracterizing the measured variables as actual causal variables. *SD* and fractal scaling are measurements commonly thought to be essential state variables in postural control. They may reflect contributions from a limited subset of actual control parameters. Certainly, *SD* and fractal exponents are not inherently physiological features but emergent properties of the postural task. However, actual control parameters may be no less emergent from task constraints—one of the rare agreements between current cognitivist theorizing about visual attention [63] and long-standing views in ecological psychology [64]. So, although the emergent control may not have the same labels for its control parameters, similar observed relationships could explain a host of previous results, as discussed above.

Visually fixating brings a prestressed quiet stance into one with informational coupling with the visual stimulus. Past work has repeatedly implicated fractal fluctuations in the head and upper torso for using visual information to organize action [28,29,65–68]. Visual inspection of IRF plots indicated rare instances of effects from or responses from CoM fractality on or to *SD* (1 trial in the 50-, 135-, and 305-cm conditions), but the regression modeling indicated no stable relationship. So, the absence of significant IRF relationships for CoM-H_{fGn} on CoP-*SD* is puzzling. However, past evidence suggests that fluctuations in the upper body moderate the use of visual information beyond and possibly in collaboration with the retina's microsaccades. CoP and movements of the upper extremities exhibit a close mutual predictive relationship in fractal and multifractal fluctuations even without involving a significant role of torso fluctuations [30,31]. Indeed, should tensegrity-themed metaphors for the movement system be apt [18], then we can expect relatively less local relationships, and CoM may be one of the multiple intermediary links in the anatomical change that need not always participate in controlling posture. Fuller-body set of measurements may allow clearer portrayal of causal relationships knitting retinal fluctuations with CoP fluctuations.

Supplementary materials

Dataset 1. DFA exponents used for VAR analysis.

Table S1. *Mean±s.e.m.* values of H_{fGn} yielded by DFA for the original (unshuffled) and a shuffled version of each CoM SED and CoP PED time series, and coefficients of paired samples *t*-tests comparing the two.

Table S2. Regression coefficients for all effects for the eyes-closed condition.

Table S3. Regression coefficients by the eyes-open conditions for the effects and interactions of Segment, Trial, Response(CoP-H_{fGn}), and Response(CoP-*SD*) without specific pairwise interactions.

Table S4. Regression coefficients by the eyes-open conditions for interactions of Segment, Trial, Impulse(CoP-H_{fGn}), and Impulse(CoP-*SD*) without specific pairwise interactions.

Table S5. Regression coefficients by the eyes-open conditions for interactions of Segment and Trial with specific pairwise self-interactions (i.e., of prior impulses of CoP-H_{fGn} on itself, and of prior impulses of CoP-*SD* on itself).

Table S6. Regression coefficients by the eyes-open conditions for interactions of Segment and Trial with specific pairwise other-interactions (i.e., of prior impulses of CoP-H_{fGn} on later values of CoP-*SD*, and of prior impulses of CoP-*SD* on later values of CoP-H_{fGn}).

References

1. Zatsiorsky VM, Duarte M. 1999 Instant equilibrium point and its migration in standing tasks: Rambling and trembling components of the stabilogram. *Motor Control* **3**, 28–38. (doi:10.1123/mcj.3.1.28)

2. Winter DA. 1995 Human balance and posture control during standing and walking. *Gait Posture* **3**, 193–214. (doi:10.1016/0966-6362(96)82849-9)

3. Chen L-C, Metcalfe JS, Chang T-Y, Jeka JJ, Clark JE. 2008 The development of infant upright posture: Sway less or sway differently? *Exp. Brain Res.* **186**, 293–303. (doi:10.1007/s00221-007-1236-1)

4. Rajachandrakumar R, Mann J, Schinkel-Ivy A, Mansfield A. 2018 Exploring the relationship between stability and variability of the centre of mass and centre of pressure. *Gait Posture* **63**, 254–259. (doi:10.1016/j.gaitpost.2018.05.008)

5. Shinbrot T, Muzzio FJ. 2001 Noise to order. *Nature* **410**, 251–258. (doi:10.1038/35065689)

6. Turing AM. 1990 The chemical basis of morphogenesis. *Bull. Math. Biol.* **52**, 153–197. (doi:10.1007/BF02459572)

7. Montesano G, Crabb DP, Jones PR, Fogagnolo P, Digiuni M, Rossetti LM. 2018 Evidence for alterations in fixational eye movements in glaucoma. *BMC Ophthalmol.* **18**, 191. (doi:10.1186/s12886-018-0870-7)

8. Meyberg S, Sinn P, Engbert R, Sommer W. 2017 Revising the link between microsaccades and the spatial cueing of voluntary attention. *Vision Res.* **133**, 47–60. (doi:10.1016/j.visres.2017.01.001)

9. Martinez-Conde S, Otero-Millan J, Macknik SL. 2013 The impact of microsaccades on vision: Towards a unified theory of saccadic function. *Nat. Rev. Neurosci.* **14**, 83–96. (doi:10.1038/nrn3405)

10. Murnaghan CD, Carpenter MG, Chua R, Inglis JT. 2016 Keeping still doesn't "make sense": Examining a role for movement variability by stabilizing the arm during a postural control task. *J. Neurophysiol.* **117**, 846–852. (doi:10.1152/jn.01150.2015)

11. Stoffregen TA, Pagulayan RJ, Bardy BG, Hettinger LJ. 2000 Modulating postural control to facilitate visual performance. *Hum. Mov. Sci.* **19**, 203–220. (doi:10.1016/S0167-9457(00)00009-9)

12. Stoffregen TA. 2010 Affordances as properties of the animal-environment system. *Ecol. Psychol.* **15**, 115–134. (doi:10.1207/S15326969ECO1502_2)

13. Stoffregen TA, Smart LJ, Bardy BG, Pagulayan RJ. 1999 Postural stabilization of looking. *J. Exp. Psychol. Hum. Percept. Perform.* **25**, 1641–1658. (doi:10.1037/0096-1523.25.6.1641)

14. Jaschinski W. 2002 The proximity-fixation-disparity curve and the preferred viewing distance at a visual display as an indicator of near vision fatigue. *Optom. Vis. Sci.* **79**, 158–168.

15. Jaschinski-Kruza W. 1991 Eyestrain in VDU users: Viewing distance and the resting position of ocular muscles. *Hum. Factors* **33**, 69–83. (doi:10.1177/001872089103300106)

16. Párraga CA, Troscianko T, Tolhurst DJ. 2002 Spatiochromatic properties of natural images and human vision. *Curr. Biol.* **12**, 483–487. (doi:10.1016/S0960-9822(02)00718-2)

17. Schleip R, Mechsner F, Zorn A, Klingler W. 2014 The bodywide fascial network as a sensory organ for haptic perception. *J. Mot. Behav.* **46**, 191–193. (doi:10.1080/00222895.2014.880306)

18. Turvey MT, Fonseca ST. 2014 The medium of haptic perception: A tensegrity hypothesis. *J. Mot. Behav.* **46**, 143–187. (doi:10.1080/00222895.2013.798252)

19. Cabe PA. 2018 All perception engages the tensegrity-based haptic medium. *Ecol. Psychol.* **31**, 1–13. (doi:10.1080/10407413.2018.1526037)

20. Ingber DE. 2006 Cellular mechanotransduction: Putting all the pieces together again. *FASEB J.* **20**, 811–827. (doi:10.1096/fj.05-5424rev)

21. Nelson CM, Jean RP, Tan JL, Liu WF, Sniadecki NJ, Spector AA, Chen CS. 2005 Emergent patterns of growth controlled by multicellular form and mechanics. *Proc. Natl. Acad. Sci. U. S. A.* **102**, 11594–11599. (doi:10.1073/pnas.0502575102)

22. Ingber DE. 2010 From cellular mechanotransduction to biologically inspired engineering. *Ann. Biomed. Eng.* **38**, 1148–1161. (doi:10.1007/s10439-010-9946-0)

23. Ingber DE. 2008 Tensegrity-based mechanosensing from macro to micro. *Prog. Biophys. Mol. Biol.* **97**, 163–179. (doi:10.1016/j.pbiomolbio.2008.02.005)

24. Hajnal A, Clark JD, Doyon JK, Kelty-Stephen DG. 2018 Fractality of body movements predicts perception of affordances: Evidence from stand-on-ability judgments about slopes. *J. Exp. Psychol. Hum. Percept. Perform.* **44**, 836–841. (doi:10.1037/xhp0000510)

25. Doyon JK, Hajnal A, Surber T, Clark JD, Kelty-Stephen DG. 2019 Multifractality of posture modulates multisensory perception of stand-on-ability. *PLoS One* **14**, e0212220. (doi:10.1371/journal.pone.0212220)

572 26. Palatinus Z, Dixon JA, Kelty-Stephen DG. 2013 Fractal fluctuations in quiet standing
573 predict the use of mechanical information for haptic perception. *Ann. Biomed. Eng.* **41**,
574 1625–1634. (doi:10.1007/s10439-012-0706-1)

575 27. Palatinus Z, Kelty-Stephen DG, Kinsella-Shaw J, Carello C, Turvey MT. 2014 Haptic
576 perceptual intent in quiet standing affects multifractal scaling of postural fluctuations. *J.*
577 *Exp. Psychol. Hum. Percept. Perform.* **40**, 1808–1818. (doi:10.1037/a0037247)

578 28. Mangalam M, Chen R, McHugh TR, Singh T, Kelty-Stephen DG. 2020 Bodywide
579 fluctuations support manual exploration: Fractal fluctuations in posture predict
580 perception of heaviness and length via effortful touch by the hand. *Hum. Mov. Sci.* **69**,
581 102543. (doi:10.1016/j.humov.2019.102543)

582 29. Mangalam M, Kelty-Stephen DG. 2020 Multiplicative-cascade dynamics supports
583 whole-body coordination for perception via effortful touch. *Hum. Mov. Sci.* **70**, 102595.
584 (doi:10.1016/j.humov.2020.102595)

585 30. Mangalam M, Carver NS, Kelty-Stephen DG. 2020 Global broadcasting of local fractal
586 fluctuations in a bodywide distributed system supports perception via effortful touch.
587 *Chaos, Solitons & Fractals* **135**, 109740. (doi:10.1016/j.chaos.2020.109740)

588 31. Mangalam M, Carver NS, Kelty-Stephen DG. 2020 Multifractal signatures of perceptual
589 processing on anatomical sleeves of the human body. *bioRxiv* , 091702.
590 (doi:10.1101/2020.05.12.091702)

591 32. Lee I-C, Pacheco MM, Newell KM. 2019 The precision demands of viewing distance
592 modulate postural coordination and control. *Hum. Mov. Sci.* **66**, 425–439.
593 (doi:https://doi.org/10.1016/j.humov.2019.05.019)

594 33. Fiorelli CM, Polastri PF, Rodrigues ST, Baptista AM, Penedo T, Pereira VAI, Simieli L,
595 Barbieri FA. 2017 Gaze position interferes in body sway in young adults. *Neurosci. Lett.*
596 **660**, 130–134. (doi:10.1016/j.neulet.2017.09.008)

597 34. Lê T-T, Kapoula Z. 2008 Role of ocular convergence in the Romberg quotient. *Gait*
598 *Posture* **27**, 493–500. (doi:10.1016/j.gaitpost.2007.06.003)

599 35. Collins JJ, De Luca CJ. 1993 Open-loop and closed-loop control of posture: A random-
600 walk analysis of center-of-pressure trajectories. *Exp. Brain Res.* **95**, 308–318.
601 (doi:10.1007/BF00229788)

602 36. Collins JJ, De Luca CJ. 1995 Upright, correlated random walks: A statistical-
603 biomechanics approach to the human postural control system. *Chaos An Interdiscip. J.*
604 *Nonlinear Sci.* **5**, 57–63. (doi:10.1063/1.166086)

605 37. Gilfriche P, Deschodt-Arsac V, Blons E, Arsac LM. 2018 Frequency-specific fractal
606 analysis of postural control accounts for control strategies. *Front. Physiol.* **9**, 293.
607 (doi:10.3389/fphys.2018.00293)

608 38. Duarte M, Sternad D. 2008 Complexity of human postural control in young and older
609 adults during prolonged standing. *Exp. Brain Res.* **191**, 265–276. (doi:10.1007/s00221-
610 008-1521-7)

611 39. Duarte M, Zatsiorsky VM. 2001 Long-range correlations in human standing. *Phys. Lett.*
612 *A* **283**, 124–128. (doi:10.1016/S0375-9601(01)00188-8)

613 40. Zatsiorsky V, Seluyanov V. 1985 Estimation of the mass and inertia characteristics of
614 the human body by means of the best predictive regression equations. *Biomechanics*
615 **IX**-**B**, 233–239.

616 41. Peng C-K, Buldyrev S V, Havlin S, Simons M, Stanley HE, Goldberger AL. 1994 Mosaic
617 organization of DNA nucleotides. *Phys. Rev. E* **49**, 1685–1689.
618 (doi:10.1103/PhysRevE.49.1685)

619 42. Peng C-K, Havlin S, Stanley HE, Goldberger AL. 1995 Quantification of scaling
620 exponents and crossover phenomena in nonstationary heartbeat time series. *Chaos An*
621 *Interdiscip. J. Nonlinear Sci.* **5**, 82–87. (doi:10.1063/1.166141)

622 43. Sims CA. 1980 Macroeconomics and reality. *Econometrica* **48**, 1–48.
623 (doi:10.2307/1912017)

624 44. Lutkepohl H. 2007 *New Introduction to Multiple Time Series Analysis*. New York, NY:
625 Springer.

626 45. Hatemi-J A. 2004 Multivariate tests for autocorrelation in the stable and unstable VAR
627 models. *Econ. Model.* **21**, 661–683. (doi:10.1016/j.econmod.2003.09.005)

628 46. Pfaff B, Stigler M, Pfaff MB. 2018 Package 'vars'. *R Packag. version 1.5-3*

629 47. Singer JD, Willett JB. 2003 *Applied Longitudinal Analysis: Modeling Change and Event*
630 *Occurrence*. New York, NY: Oxford University Press.

631 48. Pinheiro J, Bates D, DebRoy S, Sarkar D, Team RC. 2018 nlme: Linear and nonlinear
632 mixed effects models. *R Packag. version 3.1-137*

633 49. Zatsiorsky VM, Duarte M. 2000 Rambling and trembling in quiet standing. *Motor*
634 *Control* **4**, 185–200. (doi:10.1123/mcj.4.2.185)

635 50. Ferronato PAM, Barela JA. 2011 Age-related changes in postural control: Rambling and
636 trembling trajectories. *Motor Control* **15**, 481–493. (doi:10.1123/mcj.15.4.481)

637 51. Yamagata M, Popow M, Latash ML. 2019 Beyond rambling and trembling: Effects of
638 visual feedback on slow postural drift. *Exp. Brain Res.* **237**, 865–871.
639 (doi:10.1007/s00221-019-05470-w)

640 52. Kapoula Z, Lê T-T. 2006 Effects of distance and gaze position on postural stability in
641 young and old subjects. *Exp. Brain Res.* **173**, 438–445. (doi:10.1007/s00221-006-0382-
642 1)

643 53. Kuznetsov N, Wallot S. 2011 Effects of accuracy feedback on fractal characteristics of
644 time estimation. *Front. Integr. Neurosci.* **5**, 62. (doi:10.3389/fnint.2011.00062)

645 54. Kelty-Stephen DG, Dixon JA. 2014 Interwoven fluctuations during intermodal
646 perception: Fractality in head sway supports the use of visual feedback in haptic
647 perceptual judgments by manual wielding. *J. Exp. Psychol. Hum. Percept. Perform.* **40**,
648 2289–2309. (doi:10.1037/a0038159)

649 55. Stephen DG, Hajnal A. 2011 Transfer of calibration between hand and foot: Functional
650 equivalence and fractal fluctuations. *Attention, Perception, Psychophys.* **73**, 1302–
651 1328. (doi:10.3758/s13414-011-0142-6)

652 56. Hagio K, Obata H, Nakazawa K. 2018 Effects of breathing movement on the reduction
653 of postural sway during postural-cognitive dual tasking. *PLoS One* **13**, e0197385.
654 (doi:10.1371/journal.pone.0197385)

655 57. Thurner S, Mittermaier C, Ehrenberger K. 2002 Change of complexity patterns in
656 human posture during aging. *Audiol. Neurotol.* **7**, 240–248. (doi:10.1159/000063740)

657 58. Lipsitz LA. 2002 Dynamics of stability: The physiologic basis of functional health and
658 frailty. *Journals Gerontol. Ser. A* **57**, B115–B125. (doi:10.1093/gerona/57.3.B115)

659 59. Ko J-H, Newell KM. 2016 Aging and the complexity of center of pressure in static and
660 dynamic postural tasks. *Neurosci. Lett.* **610**, 104–109.
661 (doi:10.1016/j.neulet.2015.10.069)

662 60. Priplata A, Niemi J, Salen M, Harry J, Lipsitz LA, Collins JJ. 2002 Noise-enhanced
663 human balance control. *Phys. Rev. Lett.* **89**, 238101.
664 (doi:10.1103/PhysRevLett.89.238101)

665 61. Priplata AA, Niemi JB, Harry JD, Lipsitz LA, Collins JJ. 2003 Vibrating insoles and
666 balance control in elderly people. *Lancet* **362**, 1123–1124. (doi:10.1016/S0140-
667 6736(03)14470-4)

668 62. Kelty-Stephen DG, Dixon JA. 2013 Temporal correlations in postural sway moderate
669 effects of stochastic resonance on postural stability. *Hum. Mov. Sci.* **32**, 91–105.
670 (doi:10.1016/j.humov.2012.08.006)

671 63. Vecera SP, Cosman JD, Vatterott DB, Roper ZJJ. 2014 The control of visual attention:
672 Toward a unified account. In *The Psychology of Learning and Motivation* (ed BH Ross),
673 pp. 303–347. Burlington, MA: Academic Press.

674 64. Bardy BG, Marin L, Stoffregen TA, Bootsma RJ. 1999 Postural coordination modes
675 considered as emergent phenomena. *J. Exp. Psychol. Hum. Percept. Perform.* **25**,
676 1284–1301. (doi:10.1037/0096-1523.25.5.1284)

677 65. Teng DW, Eddy CL, Kelty-Stephen DG. 2016 Non-visually-guided distance perception
678 depends on matching torso fluctuations between training and test. *Attention,*
679 *Perception, Psychophys.* **78**, 2320–2328. (doi:10.3758/s13414-016-1213-5)

680 66. Eddy CL, Kelty-Stephen DG. 2015 Nesting of focal within peripheral vision promotes
681 interactions across nested time scales in head sway: Multifractal evidence from
682 accelerometry during manual and walking-based fitts tasks. *Ecol. Psychol.* **27**, 43–67.
683 (doi:10.1080/10407413.2015.991663)

684 67. Bell C, Carver N, Zbaracki J, Kelty-Stephen D. 2019 Nonlinear amplification of
685 variability through interaction across scales supports greater accuracy in manual
686 aiming: Evidence from a multifractal analysis with comparisons to linear surrogates in
687 the Fitts task. *Front. Physiol.* **10**, 998. (doi:10.3389/fphys.2019.00998)

688 68. Carver NS, Bojovic D, Kelty-Stephen DG. 2017 Multifractal foundations of visually-
689 guided aiming and adaptation to prismatic perturbation. *Hum. Mov. Sci.* **55**, 61–72.
690 (doi:10.1016/j.humov.2017.07.005)

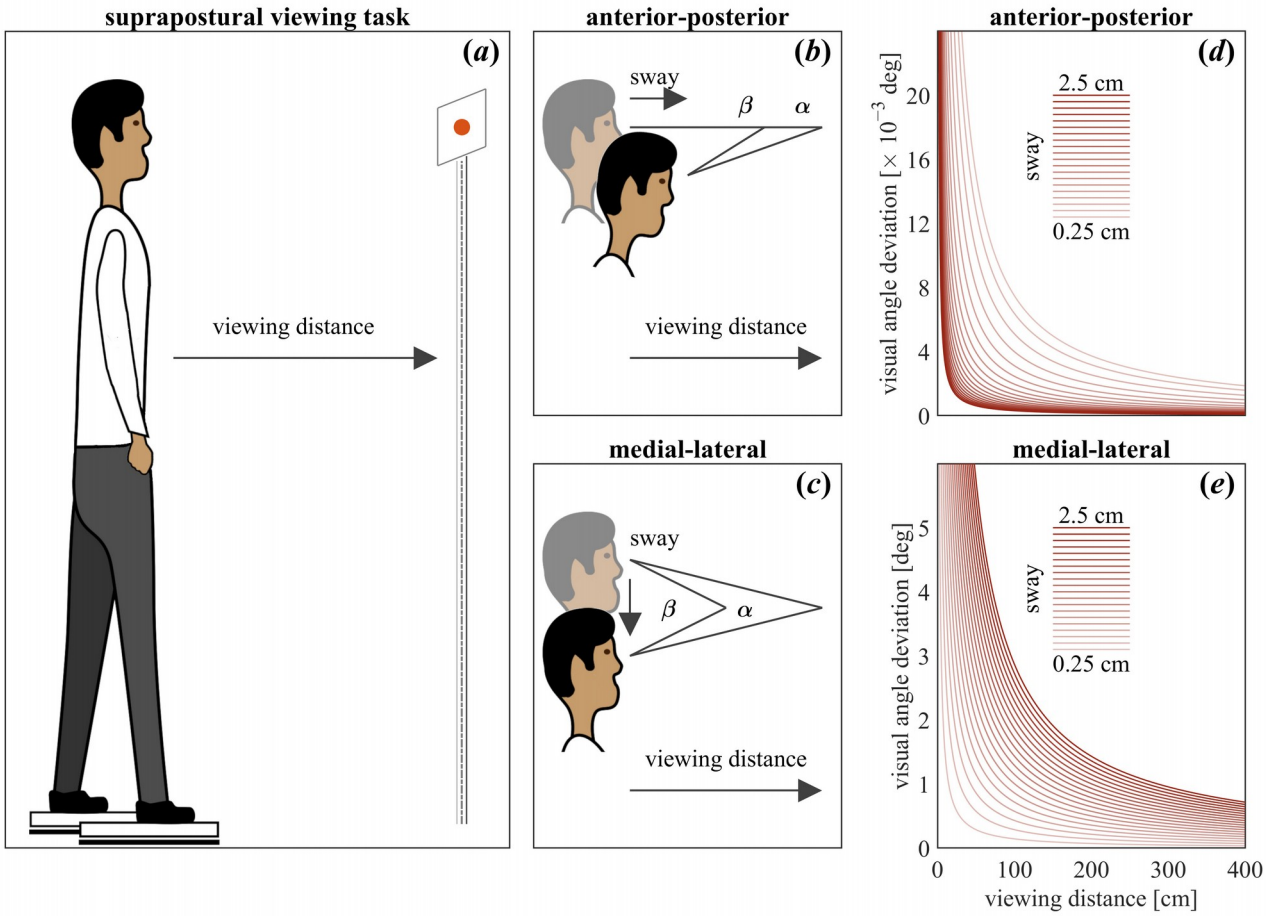

Figure 1. Schematic of the task and effects of eye-to-target distance on postural sway. (*a*) The suprapostural viewing task of standing quietly with the eyes fixated at a distant visual element. (*b*, *c*) Visual angle gain for short vs. long eye-to-target distances along the anterior-posterior (AP) and medial-lateral (ML) axes. (*d*, *e*) Visual angle gain as a function of eye-to-target distance for different sway magnitudes. Closer targets increase *AP* sway, whereas farther targets increase *ML* sway.

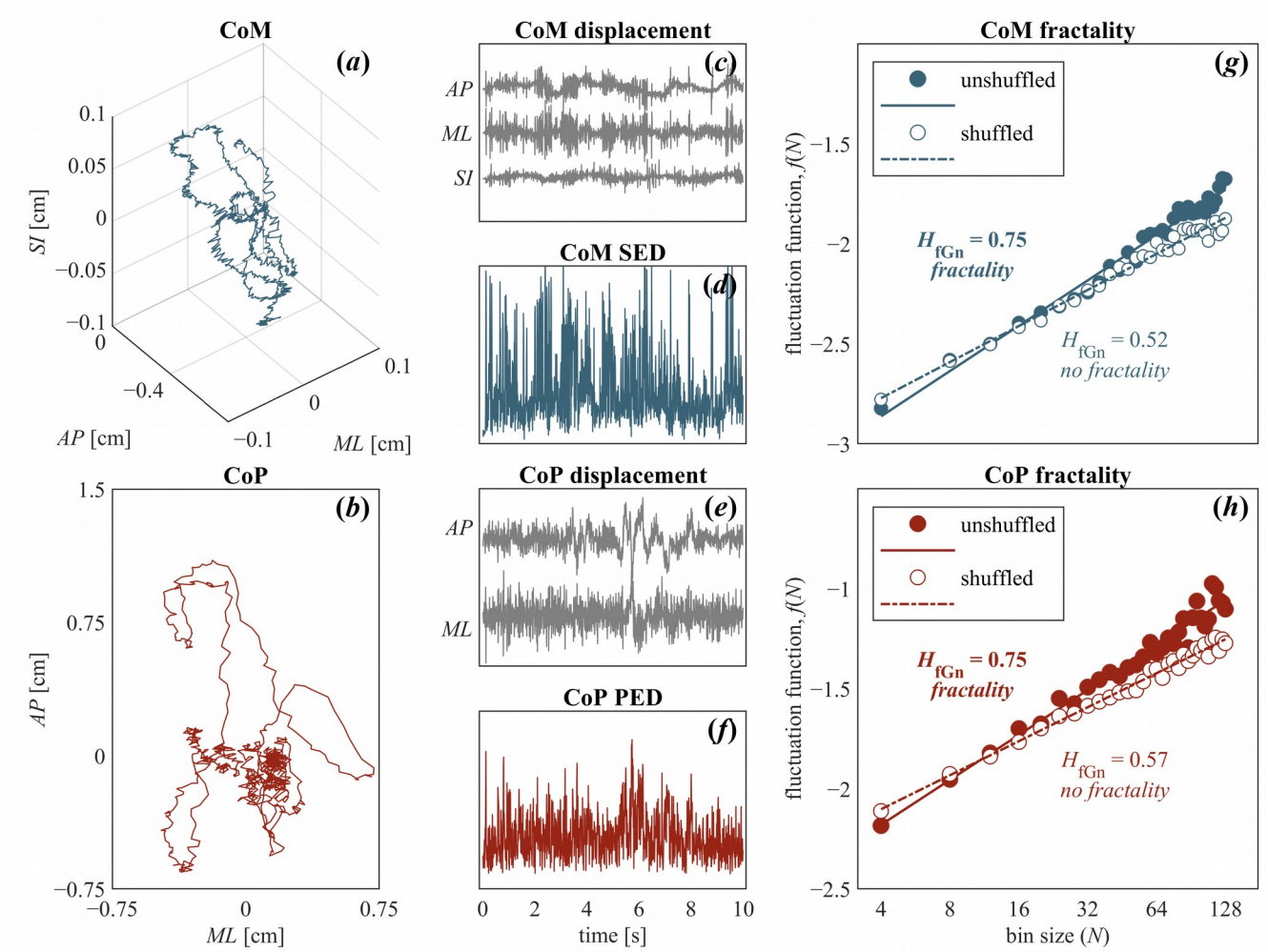

Figure 2. An overview of the detrended fluctuation analysis (DFA). (*a*, *b*) CoM and CoP in a representative 10 s segment. (*c* to *f*) CoM displacement along the medial-lateral (ML), anterior-posterior (AP), and superior-inferior (SI) axes; CoM SED series; CoP displacement along the ML, AP, and SI axes; CoP PED series. (*g*, *h*) Log-log plots of fluctuation function, f(*N*), vs. bin size (*N*), reflecting the fractal scaling exponent, H_{fGn}, yielded by DFA. Solid circles and solid trend lines represent *f*(*N*) for the original (unshuffled) series; open circles and dashed trend lines represent *f*(*N*) for a shuffled version of the original series.

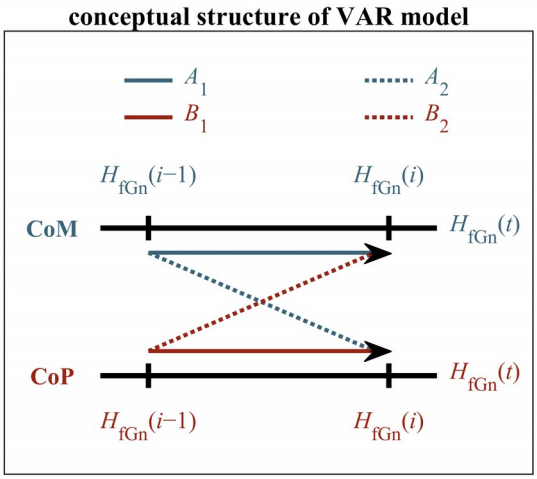

Figure 3. An overview of the vector autoregressive (VAR) analysis. VAR analysis was used to model the diffusion of fractal fluctuations across the body, as a time series of segment-by-segment values of CoM-H_{fGn}, CoP-H_{fGn}, and CoP-*SD*. Black arrows indicate the effects of H_{fGn} in the previous segment on H_{fGn} in the current segment.

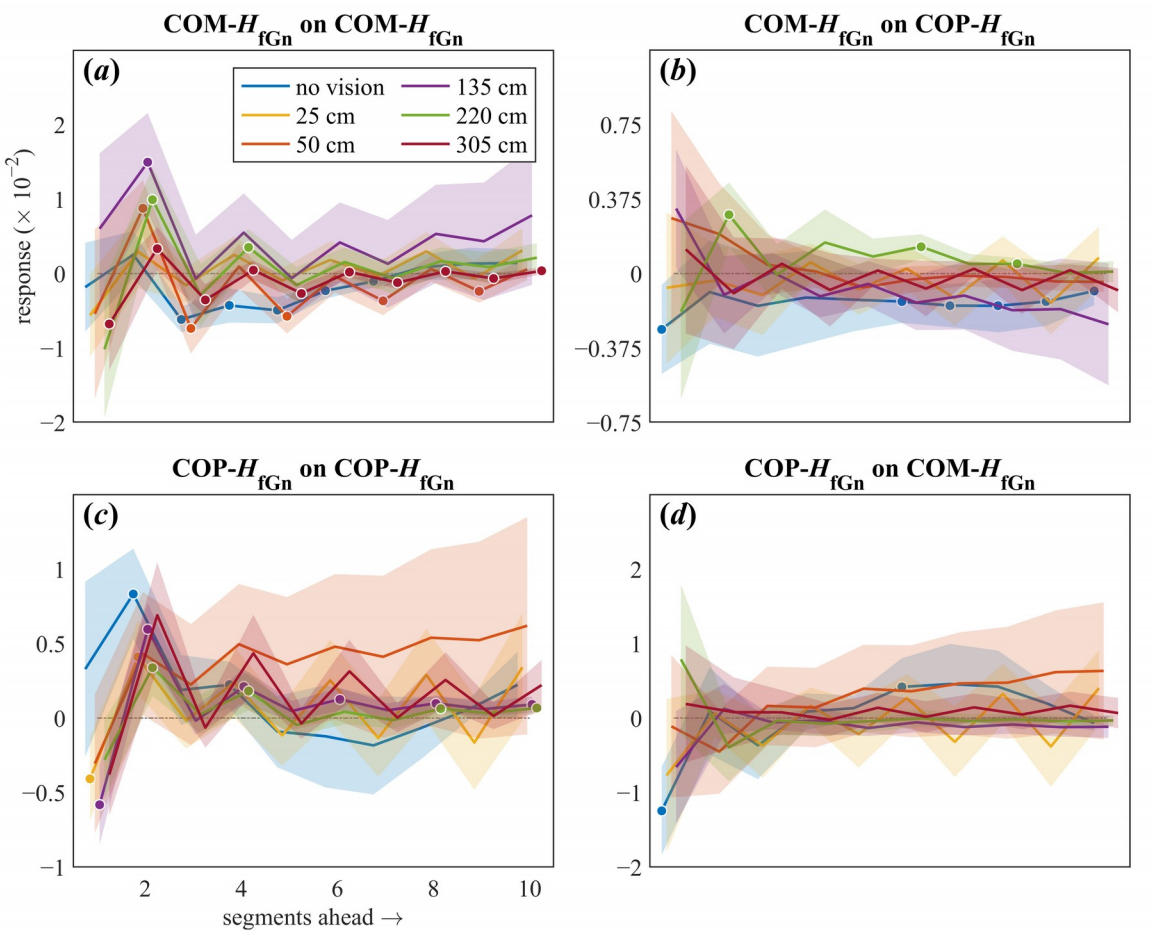

Figure 4. IRFs predicting the responses over ten segments ahead to an impulse in the current segment for each viewing condition. (*a*) CoM-H_{fGn} on CoM-H_{fGn}. (*b*) CoM-H_{fGn} on CoP-H_{fGn}. (*c*) CoP-H_{fGn} on CoP-H_{fGn}. (*d*) CoP-H_{fGn} on CoM-H_{fGn}. Shaded areas indicate *mean*±1*s.e.m.* of trial averages across all participants (n = 15). Solid circles indicate statistically significant (p < 0.01) responses to an impulse in the l^{th} segment. The curves eventually approach zero, indicating that impulse-responses weakened over subsequent segments and eventually diminished completely.

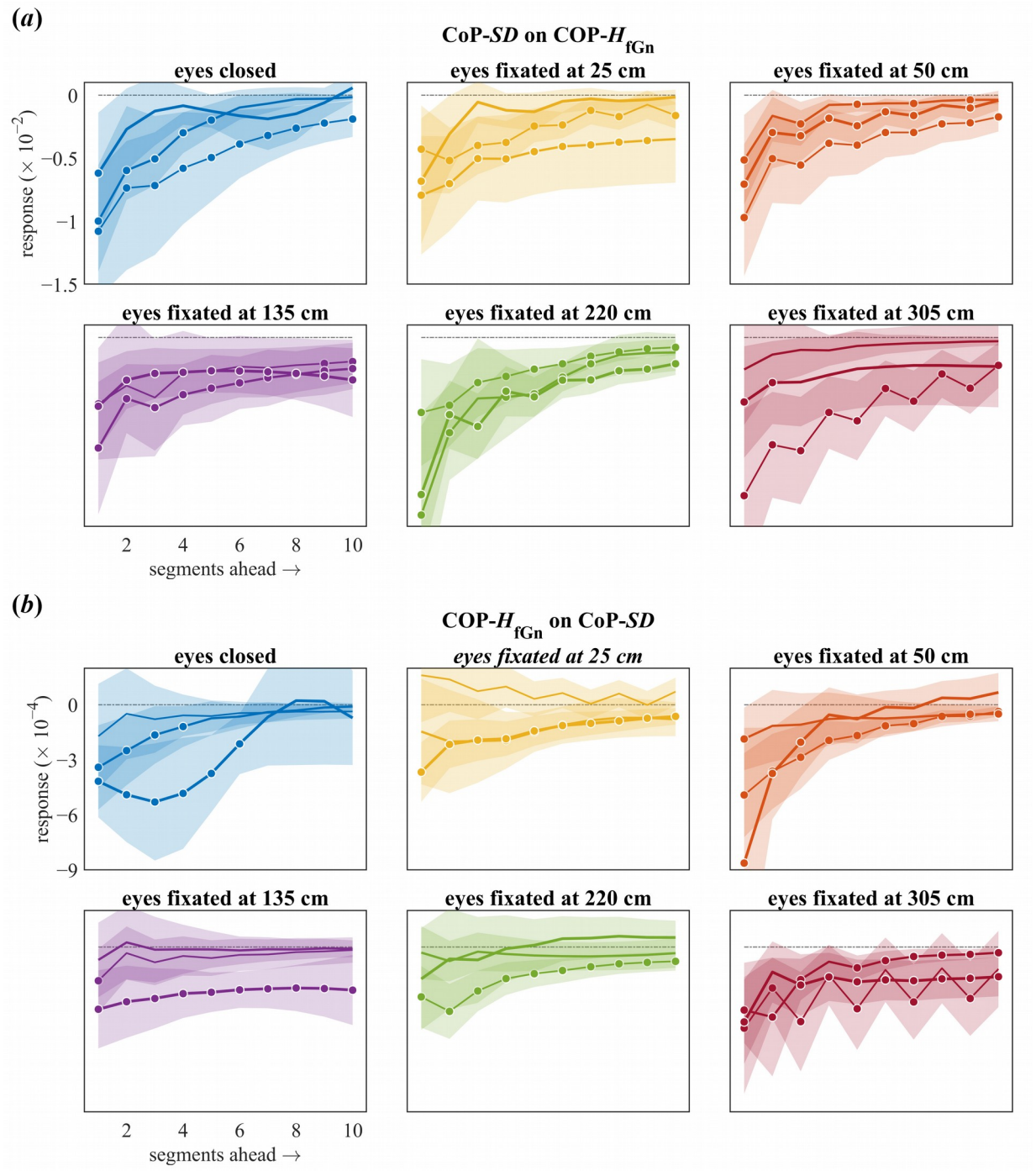

Figure 5. IRFs predicting the responses over ten segments ahead to an impulse in the current segment for each trial for each viewing condition. (*a*) CoP-*SD* on CoP-H_{fGn}. (*b*) CoP-H_{fGn} on CoP-*SD*. Line widths encode trial order (thin: trial-1; medium: trial-2; thick: trial-3). Shaded areas indicate *mean*±1*s.e.m.* of trial averages across all participants (n = 15). Solid circles indicate statistically significant (p < 0.01) responses to an impulse in the i^{th} segment. The curves eventually approach zero, indicating that impulse-responses weakened over subsequent segments and eventually diminished completely.